

THERMAL DIFFUSIVITY/CONDUCTIVITY OF IRRADIATED MONOLITHIC CVD-SiC - G. E. Youngblood, D. J. Senior and R. H. Jones (Pacific Northwest National Laboratory)*

OBJECTIVE

The primary objective of this task is to assess the thermal conduction properties of SiC before and after irradiation and after various high temperature heat treatments. Analytic models will be used to describe the fundamental behavior of the thermal conduction process in SiC as a function of microstructural properties as well as temperature and radiation dose.

SUMMARY

Several thermal diffusivity disc samples of high purity CVD-SiC were neutron-irradiated to equivalent doses of about 5-8 dpa-SiC at temperatures from 252 up to 800°C. For this temperature range, the degradation in the thermal diffusivity ranged from about 95% down to 89%, respectively. The reciprocal thermal diffusivity method was used to estimate the phonon mean free paths and defect concentrations before and after the irradiations for these materials. Even though the CVD-SiC material is an excellent monitor of certain neutron irradiation effects, the degradation in the thermal diffusivity (conductivity) appears to be more than a factor of two greater than predicted by recent theoretical model simulations.

PROGRESS AND STATUS

Introduction

A SiC material is exceptionally useful for monitoring some engineering aspects of neutron irradiation. For instance, in 1972 Price developed a method whereby SiC could be used to estimate the temperature inside a capsule during irradiation in a nuclear reactor by monitoring the recovery of its volume swelling after a series of high temperature anneals [1]. In 1995, a similar but more sensitive method for estimating the capsule irradiation temperature was examined at PNNL where the thermal diffusivity recovery rather than the volume swelling recovery was monitored also after a series of high temperature anneals [2]. This was possible because in SiC the thermal conductivity is determined by lattice or phonon conductivity, and in high purity SiC the phonon conductivity is extremely sensitive to the number of lattice imperfections. In high purity SiC neutron-irradiated at moderate temperatures (200-800°C), the lattice imperfections consist primarily of radiation-induced point defects (vacancies and interstitials). By measuring the temperature dependence of the thermal conductivity (or diffusivity) for the irradiated SiC, the phonon mean free path can be estimated and the spacing (or concentration) of the radiation-induced point defects deduced.

Originally, the analysis method developed at PNNL was used to estimate the phonon mean free path for high purity and Be-doped SiC by examining the temperature dependence of the reciprocal thermal diffusivity [3]. In this report, the reciprocal thermal diffusivity method is used to estimate the phonon mean free path for high purity Morton CVD-SiC before and after neutron irradiation at various temperatures. Then, from the calculated phonon mean free paths the radiation point defect concentrations are estimated and compared to some recent theoretical predictions by Li, et al [4].

CVD-SiC Material

The monolithic chemical vapor deposited (CVD) SiC material is a commercial product manufactured by Morton Advanced Materials (now Rohm and Haas) [5]. In the CVD process, methyltrichlorosilane (MTS)

* Pacific Northwest National Laboratory (PNNL) is operated for the U.S. Department of Energy by Battelle Memorial Institute under contract DE-AC06-76RLO-1830.

gas is decomposed onto a carbon substrate at about 1350°C. The CVD material is extremely pure, with typical impurity concentrations of less than 5 wppm. The crystal structure is cubic (3C polytype, commonly referred to as β -SiC) so provides isotropic characteristics. The grain size is between 5 and 10 μm in the plane parallel to the substrate, but the grains are elongated in the $\langle 111 \rangle$ growth direction perpendicular to the substrate. The material is homogeneous and typically free of microcracks or other large flaws, but atomic layer stacking faults on the $\{111\}$ planes are common. There is no porosity in CVD-SiC, and the material is generally considered to be theoretically dense (approximately 3.21 g/cc). The material is stiff (elastic modulus 466 GPa), and has high chemical resistance, thermal conductivity and stability at high temperatures. Therefore, CVD-SiC makes an excellent reflective optics material or electronics substrate, and also an excellent reference material for analyzing neutron irradiation effects.

Reciprocal Thermal Diffusivity Method

The thermal conductivity (k) in SiC is determined by lattice or phonon conduction. An empirical approach, in analogy to the kinetic theory of gasses, relates k for an isotropic solid to the phonon mean free path (λ) via

$$k = 1/3VC_v\lambda \quad (1),$$

where V is the phonon group velocity and C_v is the specific heat at constant volume [6]. In turn, k also may be expressed in terms of the more easily measured thermal diffusivity of the material (α) as

$$k = \alpha\rho C_p \quad (2),$$

where C_p is the specific heat at constant pressure and ρ is the bulk density. By setting Eq. (1) = Eq. (2), the thermal diffusivity may be expressed as

$$\alpha = 1/3V\lambda \quad (3),$$

if the assumption that C_v is approximately equal to ρC_p (generally valid to within 10% up to the melting point of the material). Using $\alpha(T)$ for analysis rather than $k(T)$ eliminates the complicating issue of considering the temperature dependence of C_v . Estimating λ then becomes a diffusion problem rather than an energy transport problem. For SiC, this is important since the temperature range of interest here covers 200°C $<T<800^\circ\text{C}$ and the Debye temperature ($\theta_D = 1080\text{K}$) lies within this range [7]. The phonon group velocity, estimated from the speed at which vibrations propagate through an elastic material ($V = (E/\rho)^{1/2}$) is about 1.2×10^4 m/s for SiC and is only slightly temperature dependent. By inverting and expanding Eq. (3), the reciprocal thermal diffusivity is expressed as

$$1/\alpha = (3/V)\sum_i(1/\lambda_i) = (3/V)\{1/\lambda_o + 1/\lambda_d + 1/\lambda_p\} \quad (4),$$

where the subscripts o, d and p represent the phonon mean free paths associated with intrinsic defects, radiation-induced defects and phonon-phonon interactions, respectively. At higher temperatures ($T>\theta_D$), the phonon mean free paths for defects become temperature independent, and the temperature dependence of $1/\alpha$ will be dominated by the temperature dependence of the phonon-phonon (Umklapp) interactions. Even at temperatures somewhat below θ_D , the temperature dependence of λ_o and λ_d can be considered temperature independent if the temperature dependence of λ_p is described by

$$\lambda_p = b/(T - T_o) \quad (5),$$

where b is a constant and $T_o = \theta_D/3 = 360\text{K}$ for SiC. Substituting Eq. (5) into Eq. (4),

$$1/\alpha = (3/V)\{1/\lambda_o + 1/\lambda_d - T_o/b + T/b\} = A + B(T). \quad (6),$$

where $A = (3/V)\{1/\lambda_o + 1/\lambda_d - T_o/b\}$ (7a)

and $B = 3/Vb$ (7b)

If the distribution of the intrinsic and the radiation-induced point defects is assumed to be uniform, the cubic volume λ^3 surrounding each defect is given by a_o^3/NX where a_o is the lattice parameter for β -SiC (0.436 nm), $N = 8$ is the number of atoms in the unit cell defined by a_o , and X is the fractional concentration of point defects (intrinsic plus radiation-induced). Then the defect inverse mean free path ($1/\lambda$) can be calculated from Eqs. (7a) and (7b) by

$$1/\lambda = 1/\lambda_o + 1/\lambda_d = AV/3 + T_o/b \quad (8),$$

and the defect concentration (X) is

$$X = (1/\lambda)^3 a_o^3 / N \quad (9)$$

Irradiation and Test Conditions

The thermal diffusivity of several unirradiated or irradiated CVD-SiC discs (9.5 mm dia. X 2.5 mm thick) was measured simultaneously in air as a function of temperature up to about 400°C by the laser flash method described previously [8]. Unirradiated samples on which the thermal diffusivity had already been measured were then irradiated in the HFIR reactor at ORNL as part of the JUPITER 11J-12J and 14J test series. The samples were irradiated in helium-filled capsules during seven HFIR-cycles at approximately constant, but different temperatures to doses well above saturation (for SiC saturation doses typically are <1 dpa-SiC). For doses above saturation, the SiC acquires a quasi-equilibrium concentration of radiation-induced defects, mostly vacancies and interstitials. After irradiation, the thermal diffusivity was remeasured on these same samples from RT to just below the irradiation temperature. The sample temperatures were held below the irradiation temperature to prevent defect annealing during the measurements.

In Table 1, the specific irradiation conditions for each sample are listed in order of increasing irradiation temperature. Temperature control during irradiation was more difficult for the lower temperatures, so the listed irradiation temperature is end-of-run temperature after seven cycles. The sample loading and irradiation cycle operation details are given in [9a-b].

Table 1. Irradiation conditions for CVD-SiC samples tested in JUPITER 11J or 14J.

Sample ID	Test	Eq. Dose (dpa-SiC)	Irrad. Temp.* (°C)	Est. $\Delta V/V_o$ (%)	α_{irr}/α_o ($\approx k_{irr}/k_o$)
M1	11J	7.9	252 ± 19	2.6	0.044
N5	14J	5.0	310 ± 20	2.5	0.050
N6	14J	5.1	310 ± 20	2.4	0.047
N7	14J	5.2	310 ± 20	2.5	0.046
M2	11J	7.1	355 ± 33	2.3	0.067
N3	14J	6.1	480 ± 20	2.2	0.062
N1	14J	6.8	800 ± 10	1.5	0.134
N2	14J	6.9	800 ± 10	1.5	0.113

*End-of-run temperature

Results and Discussion

In Table 1, the estimated relative volume changes (radiation-induced swelling, $\Delta V/V_0$) were determined from changes in the bulk density measurements made for each disc sample. The listed swelling estimates appear to be 20-30% higher than expected for each irradiation temperature. Nevertheless, the almost linear rate of swelling decrease with increasing irradiation temperature closely follows expected swelling behavior for SiC [10]. The dimensional measurements, carried out with a micrometer, were consistent but perhaps not very precise, which might explain the 20-30% discrepancy. Also, the irradiation temperatures monitored in the 300°C capsule tended to increase slightly (20-40°C) during each cycle [9a-b].

In Figure 1, the measured $1/\alpha$ -data are graphically presented as a function of temperature (K) for each irradiated CVD-SiC sample listed in Table 1. For reference, the straight line fit to the average $1/\alpha$ -data for unirradiated CVD-SiC is shown as a solid line near the bottom of the figure.

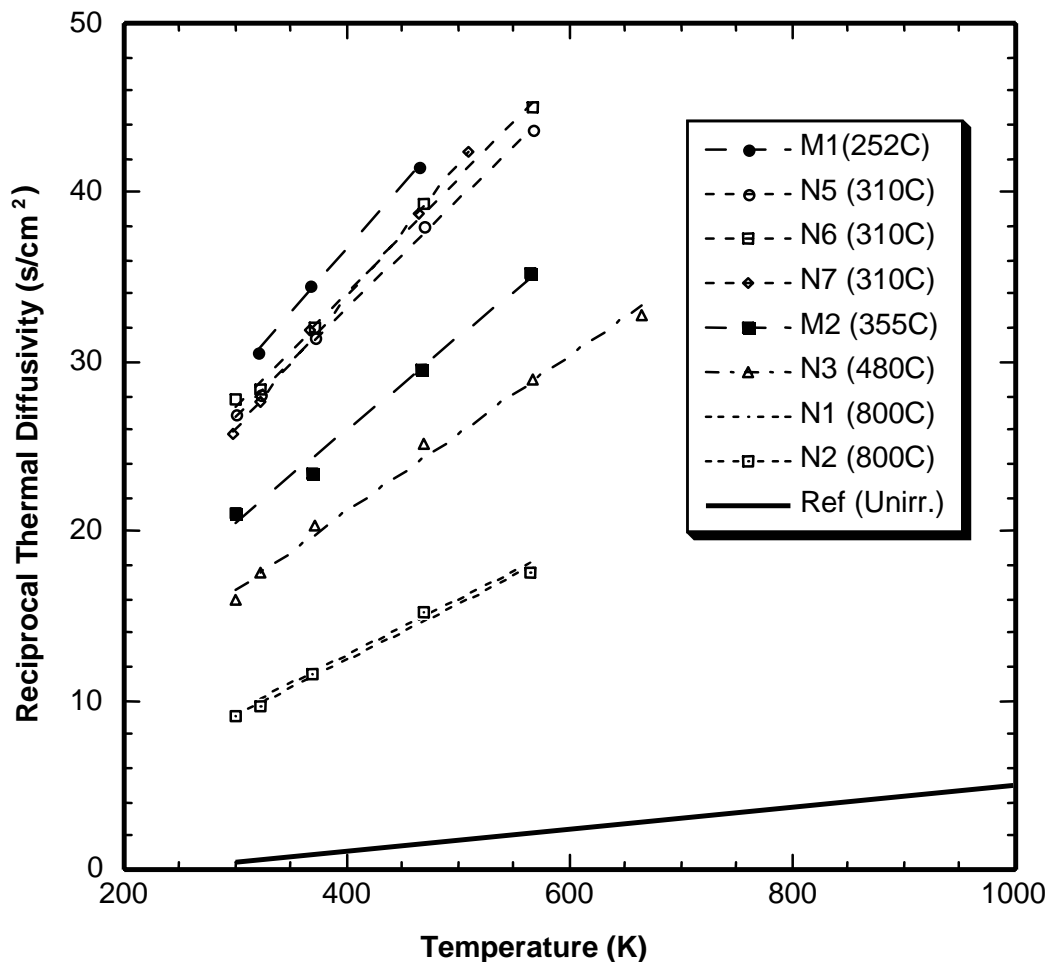


Figure 1. Comparison of the reciprocal thermal diffusivity values determined for several CVD-SiC samples irradiated at different temperatures (irradiation temperature shown in parenthesis) with reference values determined for unirradiated Morton™ CVD-SiC (solid line).

The solid reference line for CVD-SiC was calculated from the $\alpha(T)$ -curves measured before the irradiation for the six samples (N1-N7). The individual $\alpha(T)$ -curves for these unirradiated CVD-SiC samples exhibited characteristic $\sim 1/T$ temperature dependence, but also a significant spread ($\pm 20\%$). Importantly, repeated measurements on the same sample typically reproduced α -values to $\pm 5\%$. Apparently, the sample-to-sample variations were real and likely were caused by subtle differences in microstructure even though the sample discs were cut from the same plate. The $\pm 20\%$ spread in the $\alpha(T)$ -curves illustrates the importance of monitoring changes in diffusivity for the same sample before and after irradiation to properly assess changes in diffusivity due to radiation effects.

The intercepts A and slopes B, determined from a linear least squares fit to the $1/\alpha$ -data for each sample according to Eq. (6) and shown as dashed lines in Figure 1, are listed in Table 2 along with their fit correlation factor R^2 . Also listed are the λ - and X-values calculated by Eqs. (8) and (9), respectively.

Table 2. Phonon mean free path and point defect concentration calculations for CVD-SiC samples.

Sample ID	Irrad. Temp ($^{\circ}\text{C}$)	A (s/cm^2)	B ($\text{s}/\text{cm}^2\text{K}$)	R^2	λ (nm)	X (appm)
M1	252 ± 19	6.497	0.0755	0.9993	0.74	25,300
N5	310 ± 20	7.624	0.0641	0.9986	0.81	19,200
N6	310 ± 20	7.257	0.0671	0.9957	0.80	20,500
N7	310 ± 20	2.743	0.0778	0.9984	0.81	19,300
M2	355 ± 33	4.016	0.0548	0.9948	1.05	8,900
N3	480 ± 20	2.827	0.0460	0.9931	1.29	4,800
N1	800 ± 10	-0.628	0.0332	0.9893	2.21	960
N2	800 ± 10	-0.745	0.0330	0.9937	2.25	920
Ref.	-	-0.824	0.0054	0.9986	22.2	0.9

The linear fits of the $1/\alpha$ -data are exceptionally good with correlation coefficients near 0.99. The calculated λ -values decrease continuously from about 22 nm (~ 50 lattice constants) for the unirradiated reference CVD-SiC down to 0.74 nm (~ 2 lattice constants) for the sample irradiated at the lowest temperature (252°C). The calculated defect concentration for the reference sample is less than 1 appm, which is consistent with the manufacturer's value of <5 wppm impurities. The defect concentrations for the irradiated CVD-SiC samples decrease continuously from about 25,000 to 920 appm as the irradiation temperature increases from 252 to 800°C . The small concentration of intrinsic defects (<1 appm) in comparison to the extrinsic defect concentrations (>920 appm) illustrates why CVD-SiC makes an ideal irradiation damage monitor. Furthermore, these defect concentration estimates represent saturated values so should be relatively independent of dose.

In a theoretical study of the thermal properties of crystalline β -SiC, Li, et al, used a molecular dynamics simulation together with an empirical potential model to evaluate directly the heat capacity, thermal expansion and thermal conductivity for a perfect crystal, which were in excellent agreement with experimental data [4]. Then by introducing a single defect into the simulation cell (216 atoms, equivalent to 5000 appm defect concentration), they reevaluated their predictions. They found that the heat capacity and thermal expansion coefficients were little affected by the 0.5% defect concentration, in agreement with experimental data for neutron-irradiated SiC. In contrast, the thermal conductivity was markedly degraded by the dominant mechanism of defect scattering by phonons. The simulations predicted that the resulting conductivity would be essentially temperature independent from 1600K down to 436K. Interestingly, the relative conductivity degradation induced by the different types of point defects were ranked: Si interstitial at Tc site $>$ Si antisite $>$ C antisite $>$ Si vacancy $>$ C vacancy. For the 5000 appm defect concentration in β -SiC, the predicted thermal conductivity values ranged from about 15 up to 35 W/mK for the range of defect types listed above.

Listed in Table 2 for sample N3, the predicted concentration of radiation-induced defects is 4800 appm, which closely matches the 5000 appm defect concentration considered by Li, et al. However, at the irradiation temperature of 480°C the thermal conductivity calculated from the measured thermal diffusivity is only about 6.8 W/mK, more than a factor of two less than Li's conductivity predictions for any of the point defect types in SiC. An explanation for this discrepancy needs further investigation.

For engineering applications, the ratio of the irradiated to the unirradiated thermal conductivity values (k_{irr}/k_o) evaluated at the irradiation temperature is a useful quantity because k_{irr} represents the maximum degradation expected above saturation. Since neutron irradiation will have only a relatively small effect on the bulk density and heat capacity, $k_{irr}/k_o \approx \alpha_{irr}/\alpha_o$. This thermal diffusivity ratio was estimated for each irradiated CVD-SiC sample and is listed in Table 1. In Figure 2, the temperature dependence of k_{irr}/k_o is graphically presented for CVD-SiC, for the Hi-Nicalon™ and Sylramic™ composites reported earlier, and for similar values selected from the literature.

In Figure 2, the k_{irr}/k_o -data for CVD-SiC reported by Thorne, et al., Rohde, and Senor, et al. were similarly plotted in [11]. Likewise, k_{irr}/k_o -data for SiC/SiC composite made with first generation Nicalon™ CG fibers were given. The general trend is for the k_{irr}/k_o ratio to increase as the irradiation temperature increases. This trend reflects the relative dominance of temperature independent point defect phonon scattering in the lower temperature range, while the temperature dependent phonon-phonon scattering becomes relatively more important as the irradiation/test temperature increases. The curve for CVD-SiC represents the lower limit for irradiation degradation in SiC. In contrast, the phonon scattering in SiC/SiC composite materials is dominated by numerous structural defects even before irradiation, and the addition of irradiation point defects has a relatively small effect on the conductivity degradation. Thus, the curve through the Nicalon™ CG composite data marks an upper limit for the k_{irr}/k_o ratio for SiC-based materials. The new k_{irr}/k_o data for the SiC/SiC composite made with second generation Hi-Nicalon™ or Sylramic™ fiber generally fall in between the two limits.

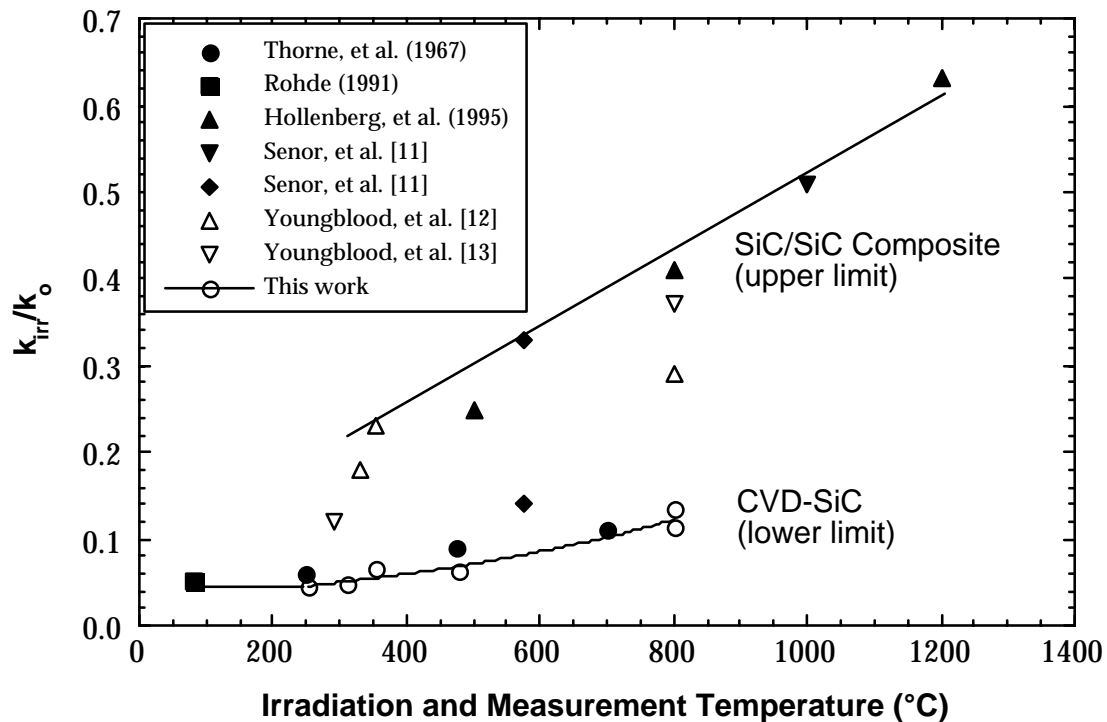


Figure 2. Conductivity degradation as a function of irradiation and test temperature for CVD-SiC and SiC/SiC composite.

FUTURE WORK

An attempt will be made to examine the kinetics of the thermal diffusivity recovery during annealing for the CVD-SiC samples irradiated at different temperatures and containing vastly different concentrations of point defects. Appropriate TEM analysis will accompany the thermal diffusivity recovery studies.

REFERENCES

- [1] J. Price, "Annealing behavior of neutron-irradiated SiC temperature monitors," *Nuclear Technology* 16, 536-542 (1972).
- [2] G. E. Youngblood, "Passive SiC irradiation temperature monitor," p. 324 in *Fusion Materials Semiannual Progress Report (FMSPR) for period ending December 31, 1995.* (DOE/ER-0313/19)
- [3] G. E. Youngblood and W. Kowbel, "Improvements of the thermal conductivity of SiCf/SiC composite," p. 107 in *ibid.*
- [4] Li, Lisa Porter and Sydney Yip, "Atomistic modeling of finite-temperature properties of crystalline β -SiC: II. Thermal conductivity and effects of point defects," *J. Nucl. Mater.* 255, 139-152 (1998).
- [5] Morton Advanced Materials, 1996. CVD Silicon Carbide, technical Publication 107, Morton Advanced Materials (now Rohm and Haas), Woburn, MA 01801.
- [6] D. R. Flynn, "Thermal conductivity of ceramics," p. 63 in *Mechanical and Thermal Properties of Ceramics*, ed. J. B. Wachtman, Jr., NBS Special Publication 303, Washington D.C., May, 1969.
- [7] J. S. Haggerty and A. Lightfoot, "Opportunities for enhancing the thermal conductivities of SiC and Si₃N₄ ceramics through improved processing," *Ceram. Eng. Sci. Proc.*, 475-487 (1996).
- [8] D. J. Senior, G. E. Youngblood, D. V. Archer and C. E. Chamberlin, "Recent progress in thermal diffusivity testing of SiC-based materials for fusion reactor applications," p. 102 in the *Proceedings of the 3rd IEA SiC/SiC Workshop, January 29-30, 1999, Cocoa Beach, Florida.*
- [9a] A. L. Qualls, "HFIR-MFE-RB-14J specimen loading listing and operational summary," p. 241 in *FMSPR for period ending June 30, 2000.* (DOE/ER-0313/28)
- [9b] M. L. Grossbeck, K. E. Lenox and M. A. Janney, "The Monbusho/U.S. experiment: HFIR-MFE-RB-11J and 12J," p. 254 in *FMSPR for period ending June 30, 1997.* (DOE/ER-0313/22)
- [10] S.J. Zinkle and L.L. Snead, "Thermophysical and mechanical properties of SiC/SiC composites," p. 93 in *FMSPR for period ending December 31, 1998.* (DOE/ER-0313/24)
- [11] D. J. Senior, G. E. Youngblood, C. E. Moore, D. J. Trimble, G. A. Newsome and J. J. Woods, "Effects of neutron irradiation on thermal conductivity of SiC-based composites and monolithic ceramics," *Fusion Technology* 30(3), 943-955 (1996).
- [12] G. E. Youngblood, D. J. Senior and R. H. Jones, "Thermal diffusivity/conductivity of irradiated Hi-Nicalon™ 2D-SiC/SiC composite," in this *FMSPR.*
- [13] G. E. Youngblood, D. J. Senior and R. H. Jones, "Thermal diffusivity/conductivity of irradiated Sylramic™ 2D-SiC/SiC composite," in this *FMSPR.*